Journal of Luminescence 198 (2018) 502–507

Contents lists available at ScienceDirect

Journal of Luminescence

journal homepage: www.elsevier.com/locate/jlumin

Entanglement in electron-nuclear spin system as immediate cause of the dependence of dephasing rate $1/T_2$ on intensity in the optical Bloch equations

I.S. Osad'ko[a,*], M.A. Mikhailov[b]

[a] Institute for Spectroscopy RAS, Moscow, Russia
[b] Moscow State Pedagogical University, Moscow, Russia

A B S T R A C T

Dephasing rate $1/T_2$ in the optical Bloch equations doesn't depend on Rabi frequency $\chi = Ed/\hbar$. It seemed true for various mechanisms responsible for optical dephasing processes. In this paper we show that entanglement of nuclear spin with electronic transition in an atom results in dependence of $1/T_2$ on χ. Rate $1/T_2(\chi)$ decreases if χ increases. This effect is able to explain experimental data on free-induction decay measured in $Pr_3{}^+$:LaF_3 crystal.

1. Introduction

The Bloch equations derived for magnetic resonance [1] play important role in optical resonance as well [2]. Physical idea enabling us to use Bloch equations for optical resonance was based on formal analogy between two-state spin system and two-level atom (molecule).

Nevertheless, some doubts emerged that the optical Bloch equations are able to describe all details of the optical resonance. Therefore, DeVoe & Brewer in their paper [3] entitled "Experimental Test of Optical Bloch Equations for Solids" decided to verify applicability of the optical Bloch equations for crystals with paramagnetic ions. Result of their measurement of free-induction decay (FID) in Pr^{3+}:LaF_3 crystal was in strong disagreement with the decay predicted by the optical Bloch equations.

Crystal Pr^{3+}:LaF_3 was chosen for FID experiments because values of $T_1 = 0.5ms$ and $T_2 = 21.7\mu s$ for this crystal were found earlier in Refs. [4,5]. Excitation of ions Pr^{3+} was realized via $^1D_2 - {}^3H_4$ transition at wave length 5925 Å during 400 µs. After that laser was switched off and light emitted by induced electronic polarization was detected. In accordance with the optical Bloch equations dependence of emission on time is described by the following function $\exp[-t/T_2 - \Delta\omega(\chi)t]\cos\omega_0 t$, where:

$$\Delta\omega(\chi) = \sqrt{(1/T_2)^2 + \chi^2(T_1/T_2)}, \quad (1)$$

is rate of the decay depending on Rabi frequency $\chi = Ed/\hbar$, and ω_0 is a resonant frequency. Eq. (1) doesn't include unknown parameters because values $T_1 = 0.5ms$ и $T_2 = 21.7\mu s$ have been measured in independent experiments earlier [4,5]. Dependence of $\Delta\omega(\chi)$ on Rabi frequency described by Eq. (1) is shown in Fig. 1 by solid line whereas the dependence measured is shown by dots.

We see strong disagreement with prediction derived from the optical Bloch equations. At small values of χ the measured function $\Delta\omega(\chi)$ is increased in accordance with the prediction of the optical Bloch equations. However, at large values of χ, the measured function $\Delta\omega(\chi)$ is increased approximately as χ instead of the dependence $\chi(T_1/T_2)^{1/2} \approx \chi(23)^{1/2}$ predicted by the optical Bloch equations.

Later Szabo and Muramoto [6] have found that FID in ruby demonstrates disagreement with Eq. (1) similar that shown in Fig. 1. It became clear that the optical Bloch equations cannot describe transient phenomena in paramagnetic crystals without serious modification in these equations.

Therefore, immediately many theories have been advanced for modification of the optical Bloch equations aimed to explain disagreement found in the experiment. Influence of Markovian [7–17] and non-Markovian [18,19] processes on the optical Bloch equations have been analyzed.

Analysis of these theories has been carried out by Berman [14,15], Javanainen [10], Szabo and Muramoto [6]. As it was pointed out by Szabo and Muramoto in accordance with analysis made by Berman and Javanainen "*...none of the numerical calculations presented so far consistently describe the data for Pr^{3+}:LaF_3*" Summing up their own analysis Szabo and Muramoto [6] pointed out «*We have found that the Gauss-Markov or random-telegraph modifications of the optical Bloch equations do not consistently describe free-induction and echo-decay measurements with a single correlation time for the assumed stochastic frequency fluctuations. It is suggested that a nonstochastic model ...may be useful to study*"

* Corresponding author.
E-mail address: osadko@isan.troitsk.ru (I.S. Osad'ko).

https://doi.org/10.1016/j.jlumin.2018.01.040
Received 6 July 2017; Received in revised form 6 November 2017; Accepted 19 January 2018
Available online 31 January 2018
0022-2313/

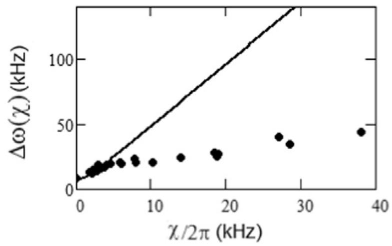

Fig. 1. Dependence on Rabi frequency calculated with the help of Eq. (1) (line) and the dependence measured in experiment [3] (dots).

Hence, all types of stochastic theories were unable to describe correctly experimental data presented in Fig. 1.

Since stochastic approaches fail to explain experimental data shown in Fig. 1 we decided to use purely dynamical approach based on a Hamiltonian of the system and quantum-mechanical calculations of dephasing rate with the help of chosen Hamiltonian. In this paper we explain essence of our dynamical model and show that the theoretical curve calculated in our theory fits experimental data shown in Fig. 1 well.

2. Hamiltonian of electron-spin system without entanglement

In accordance with Ref. [3], optical dephasing in Pr^{3+}:LaF_3 crystal results from the dipolar interaction between spin in nucleus ^{19}F and electronic transition in Pr^{3+} ion. Such electron-spin system mathematically looks similar to electron-two level (TLS) system considered in many works for a guest molecules embedded to polymer or glass. Non-perturbative theory for electron-TLS system has been developed earlier by Osad'ko [20–22]. This very theory for electron-TLS system we take as basis for our consideration of electron-spin system in paramagnetic crystals with guest ions.

The Hamiltonian of electron-spin system interacting with light we take in the following form:

$$H = H_0 + H_{phot} + H_{el-phot}, \tag{2}$$

$$H_0 = \hbar\omega_0 B^+B + \varepsilon c^+c + \hbar\Delta_0 B^+Bc^+c. \tag{3}$$

Here $B^+$and B are operators of creation and annihilation of electronic excitation, c^+ and c are operators of creation and annihilation of excitation in spin system.

Our 4-state system consists of two-level atom with two electronic states described by populations $n_{0,1}$ and two nuclear spin states with populations ρ_α and ρ_β. This 4-state system with Hamiltonian (3) is described by the diagram presented in Fig. 2

Operator $V_{e-s}^{(d)} = \hbar\Delta_0 B^+Bc^+c$ describes electron-spin interaction that is responsible for optical dephasing. Probabilities $n_0\rho_\alpha$, $n_1\rho_\alpha$, $n_0\rho_\beta$, $n_1\rho_\beta$ of finding four quantum states are products of electronic probabilities $n_{0,1}$ and spin probabilities $\rho_{\alpha,\beta}$:

$$P_0 = n_0\rho_\alpha,\ P_1 = n_1\rho_\alpha,\ P_2 = n_0\rho_\beta,\ P_3 = n_1\rho_\beta \tag{4}$$

Here $\rho_\beta = f = [1 + \exp(\varepsilon/kT)]^{-1}$, $\rho_\alpha = 1 - f$ describes spin probability in thermal equilibrium. They are independent on electronic state of Pr^{3+} ion.

Operator $V_{e-s}^{(d)} = \hbar\Delta_0 c^+cB^+B$ of the interaction is diagonal with respect to electron and spin variables. This operator is responsible for

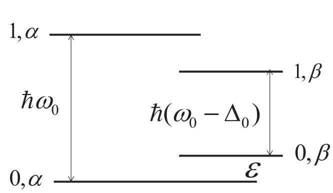

Fig. 2. Energy diagram for electron-spin system.

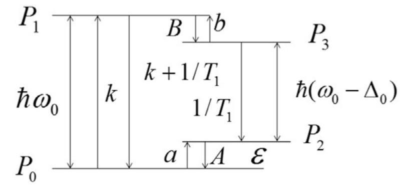

Fig. 3. Entangled electron-spin system excited by light.

appearance of optical dephasing in the system. Calculation of optical dephasing in the system which is described by Hamiltonian H_0 is presented in Appendix A. Final Eq. (A19) for optical dephasing rate in the electron-spin system depends solely on temperature via function $f = [1 + \exp(\varepsilon/kT)]^{-1}$

3. Entanglement in electron-spin system excited by light

Let us include in Hamiltonian (3) operator

$$V_{e-s}^{(off)} = V_0(c + c^+) + V_1B^+B(c + c^+). \tag{5}$$

that is off-diagonal with respect to spin operators. In presence of this operator electronic and spin variables are entangled and we arrive at the energy diagram presented in Fig. 3

Here rate constants are described by the following equations:

$$a = 2\pi\sum_{a,b} w_{0,a}(\alpha)|(V_1)_{ab}|^2\delta(\Omega_a - \Omega_b - \varepsilon/\hbar) \tag{6a}$$

$$A = 2\pi\sum_{a,b} w_{0,b}(\beta)|(V_1)_{ab}|^2\delta(\Omega_a - \Omega_b - \varepsilon/\hbar) \tag{6b}$$

$$B = 2\pi\sum_{a,b} w_{1,a}(\alpha)|(V_2)_{ab}|^2\delta(\Omega_a - \Omega_b - \varepsilon/\hbar + \Delta) \tag{6c}$$

$$b = 2\pi\sum_{a,b} w_{1,b}(\alpha)|(V_2)_{ab}|^2\delta(\Omega_a - \Omega_b - \varepsilon/\hbar + \Delta) \tag{6d}$$

Here Ω_a and Ω_b are frequencies of phonon excitations. Two left levels in Fig. 3 describe two electronic states with nucleus spin in α state. Two right levels describe the same electronic levels when nucleus is in β spin state.

If $V_{e-s}^{(off)} \neq 0$, constants a,A,b and B are not equal zero and we arrive at the following four rate equations for the populations $P_0 = P_1 = P_2 = P_3$

$$\begin{aligned}
\dot{P}_0 &= -[k(\chi) + a]P_0 + \Gamma P_1 + AP_2 + 0,\\
\dot{P}_1 &= k(\chi)P_0 - (\Gamma + B)P_1 + 0 + bP_3,\\
\dot{P}_2 &= aP_0 + 0 - AP_2 + P_3/T_1,\\
\dot{P}_3 &= 0 + BP_1 + 0 - (b + 1/T_1)P_3
\end{aligned} \tag{7}$$

Here $\Gamma = k(\chi) + 1/T_1$. Rate k of electronic excitation is given by:

$$k(\chi) = \frac{\chi^2}{2}\frac{1/T_2}{\Delta^2 + (1/T_2)^2}, \tag{8}$$

where $\Delta = \omega - \omega_0$. Rates A, a, B, b describe jumps from spin state α to spin state β and back. Probabilities P_j found from Eq. (7) cannot be written as product of electronic and spin probabilities similar to Eq. (4). Hence Eq. (7) describe evolution in time of entangled electron-nuclear spin states.

Consider the following two probabilities for spin:

$$1 - f = P_0 + P_1,\ f = P_2 + P_3 \tag{9}$$

They describe probabilities of finding spin in state α and β, respectively. Eq. (9) determines probabilities which should be inserted to Eq. (A4) for the spin density matrix in Appendix A. In such case Eq. (A4) will look as follows

$$\hat{\rho}^g = (P_0 + P_1)cc^+ + (P_2 + P_3)c^+c \tag{10}$$

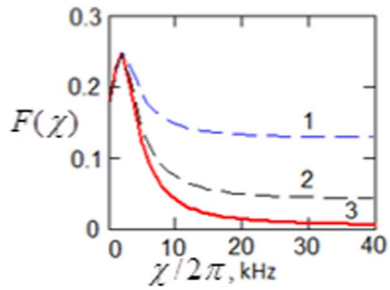

Fig. 4. Dependence of function F on Rabi frequency at A/a = 0.3 and BT_1 = 10, B/A = 1 (line 1), BT_1 = 40, B/A = 10 (line 2), BT_1 = 450, B/A = 50 (line 3).

Then we can repeat all steps in derivation presented in Appendix A. We arrive at Eq. (A19) again. However function $F = f(1-f)$ will look as follows: $F = (P_2 + P_3)(P_0 + P_1)$.

We find mathematical expression for function F = f(1 − f) after solution of four rate Eq. (7) for stationary case. The result at $bT_1 \ll 1$ looks as follows:

$$F(\chi) = f(1-f) = \frac{\left[\frac{a}{A} + \frac{k(\chi)T_1}{k(\chi)T_1 + 1 + BT_1}\left(BT_1 + \frac{B}{A}\right)\right]\left[1 + \frac{k(\chi)T_1}{k(\chi)T_1 + 1 + BT_1}\right]}{\left[1 + \frac{a}{A} + \frac{k(\chi)T_1}{k(\chi)T_1 + 1 + BT_1}\left(1 + BT_1 + \frac{B}{A}\right)\right]^2} \quad (11)$$

This function depends on Rabi frequency. Function F is shown in Fig. 4 at various values of parameter B.

Function F decreases when Rabi frequency increases. Value of rate B influences considerably on decrease of function F(χ).

4. Dependence of optical dephasing rate on Rabi frequency

Dephasing rate in the physical system whose dynamics is described by four Eq. (7) is given by:

$$\frac{1}{T_2(\chi)} = \frac{1}{2T_1} + \frac{\gamma_{ph}}{2} + \frac{\gamma_{e-s}(\chi)}{2} \quad (12)$$

Although our Hamiltonian doesn't include phonons we must take into account their contribution to the dephasing rate. Here term γ_{ph} describes contribution from phonons to optical dephasing.

We know value of dephasing rate $\frac{1}{T_2(0)} = \frac{1}{2T_1} + \frac{\gamma_{ph}}{2} + \frac{\gamma_{e-s}(0)}{2} = \frac{1}{21.7\mu s}$ at $\chi = 0$. Therefore Eq. (12) can be rewritten in the following form

$$\frac{1}{T_2(\chi)} = \frac{1}{T_2(0)} + \frac{\gamma_{e-s}(\chi)}{2} - \frac{\gamma_{e-s}(0)}{2} \quad (13)$$

Consider now dependence of optical dephasing on Rabi frequency at various values of parameter B. Inserting Eq. (A22) from Appendix A into Eq. (13) we arrive at the final expression for optical dephasing rate:

$$\frac{1}{T_2(\chi)} = \frac{1}{T_2(0)} + \gamma[I(\chi, \Delta_0/\gamma) - I(0, \Delta_0/\gamma)] \quad (14)$$

Here $I(\chi, \Delta_0/\gamma)$ is dimensionless integral described by Eq. (A22) and Eq. (A20) in Appendix A. Dependence of this integral on Rabi frequency at various values of dimensionless coupling constant Δ_0/γ is shown in Fig. 5

Let us consider a simplified version for this dimensionless integral. Integral in Eq. (A22) can be presented in the following approximate form:

$$\frac{\gamma_{e-s}}{2} = gI_0(\chi, \Delta_0/g) \approx g6.5\frac{\Delta_0^2}{\Delta_0^2 + g^2}F(\chi) \quad (15)$$

This formula is more convenient for use in practice as compared with Eq. (A22) because dependence of the integral on coupling constant is separated from the dependence on Rabi frequency. Dependence of this approximate integral $I_0(\chi, \Delta_0/g)$ on Rabi frequency at various values of coupling constant is shown in Fig. 6

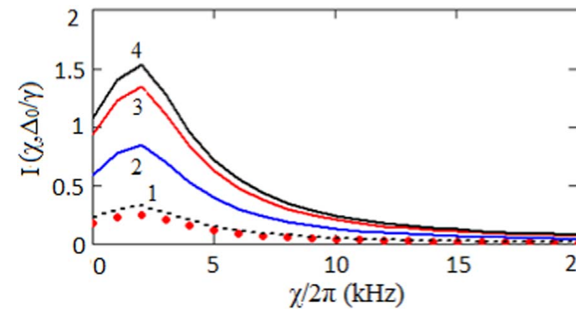

Fig. 5. Dependence of dimensionless integral $I(\chi, \Delta_0/\gamma)$ on Rabi frequency at various values of dimensionless coupling constant Δ_0/γ = 1 (1), 2 (2), 4(3), 8(4). Dots show function $F(\chi)$ calculated with the help of Eq. (11) at the following values of parameters: $B = 9 \times 10^5 s^{-1} A = 1.8 \times 10^4 s^{-1}$, $a = 5.4 \times 10^3 s^{-1}$.

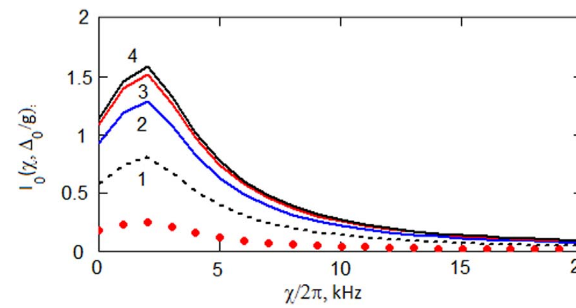

Fig. 6. Dependence of dimensionless integral $I_0(\chi, \Delta_0/g)$ on Rabi frequency at various values of dimensionless coupling constant Δ_0/γ = 1 (1), 2 (2), 4(3), 8(4). Dots show function $F(\chi)$ calculated with the help of Eq. (11) at $B = 9 \times 10^5 s^{-1} A = 1.8 \times 10^4 s^{-1}$, $a = 5.4 \times 10^3 s^{-1}$.

Curves in Figs. 5 and 6 are similar with each other. Therefore calculation of dephasing rate can be described by the following simplified expression

$$\frac{1}{T_2(\chi)} = \frac{1}{T_2(0)} + 13\frac{g}{2}\frac{\Delta_0^2}{\Delta_0^2 + g^2}[F(\chi) - F(0)] \quad (16)$$

Consider now dependence of optical dephasing on Rabi frequency at various values of parameter B. Fig. 7 shows such dependence.

At $a/A = 0$, $b = B = 0$ dephasing rate is constant because interaction with spin is switched off (line 1). At $a/A = 0.3$, BT_1, =10, $B/A = 1$ (line 2) and at $a/A = 0.3$, $BT_1 = 40$, $B/A = 4$ (line 3) dependence on Rabi frequency becomes weaker. At $a/A = 0.3$, $B = 450$, $b = 50$ (line 4) optical dephasing decreases considerably when Rabi frequency increases. This very line fits experimental data well. Hence rate B that determines influence of the excited electronic state on nucleus spin plays decisive role in decrease of dephasing rate.

Taking into account that dephasing rate $1/T_2(\chi)$ in the optical Bloch

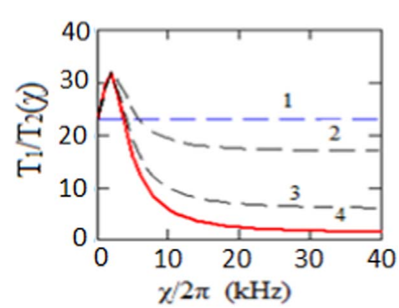

Fig. 7. Dependence of optical dephasing rate on Rabi frequency at $a/A = BT_1 = B/A = 0$ (line 1), $a/A = 0.3$, BT_1, =10, $B/A = 1$ (line 2) , $a/A = 0.3$, $BT_1 = 40$, $B/A = 4$ (line 3), $a/A = 0.3$, $BT_1 = 450$, $B/A = 50$ (line 4).

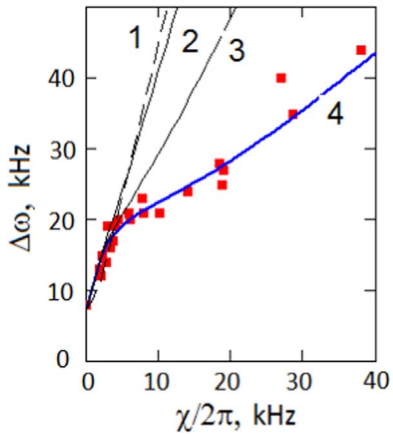

Fig. 8. Comparison of experimental data [3] (squares) with theoretical curve 4. Dashed line 1 relates to the optical Bloch equations with $T_1/T_2(0) = 23$. Other theoretical curves were calculated with the help of Eq. (11), Eq. (16) and Eq. (17) at various values of B. Curves 1,2,3 and 4 were obtained at $a/A = BT_1 = B/A = 0$ (line 1) and at $a/A = 0.3$, BT_1, =10, $B/A = 1$ (line 2) $BT_1 = 40$, $B/A = 4$ (line 3), $BT_1 = 450$, $B/A = 50$ (line 4).

equations can depend on Rabi frequency as Fig. 7 shows we obtain instead of Eq. (1) the following equation:

$$\Delta\omega(\chi) = \sqrt{[1/T_2(\chi)]^2 + \chi^2 [T_1/T_2(\chi)]} \tag{17}$$

By calculating this equation for various values of parameter B we find curves depicted in Fig. 8.

Curve 4 fits experimental data well. It was calculated with the following set of parameters: $a/A = 0.3$, $BT_1 = 450$, $B/A = 50$ and $6.5g\Delta_0^2/(g^2 + \Delta_0^2) = 2.533 \times 10^5 s^{-1}$. Since $T_1 = 0.5$ ms we can easily find the following values for parameters: $B = 9 \times 10^5 s^{-1}$, $A = 1.8 \times 10^4 s^{-1}$, $a = 5.4 \times 10^3 s^{-1}$

5. Conclusion

In contrast with all previous theoretical works we used purely dynamical quantum-mechanical approach for optical dephasing in paramagnetic crystal. We have shown that optical dephasing calculated in entangled electron-nuclear spin system manifests surprising feature: it decreases if Rabi frequency increases. This entanglement is key point of our theory for dephasing rate.

As usual, each additional dephasing mechanism increases dephasing rate. However, mechanism with entangled electron-nuclear spin system decreases rate as Fig. 8 shows. This behavior of dephasing rate enables one to explain disagreement shown in Fig. 1.

Acknowledgement

This work was supported by the Russian Science Foundation via grant 14-12-01415.

Appendix A. Derivation of the expression for dephasing time

Diagram in Fig. 2 is similar to that which describes a two-level atom interacting with so-called two-level system (TLS) of a glass. Optical dephasing in such system with TLS has already been studied in Refs. [20–22].

Rate of the electronic transition from the ground to the excited electronic state in the first nonvanishing approximation by electron-photon operator $H_{el-phot}$ is given by the following expression [22]:

$$J(\omega) = \frac{1}{2\pi}\int_{-\infty}^{\infty} e^{i(\omega-\omega_0)t - t/(2T_1)} J(t)dt, \tag{A1}$$

Function J(t) is described by the following equation: $\widehat{S}(t)$

$$J(t) = \chi^2 \mathrm{Tr}\left\{\hat{\rho}^g \exp\left(it\frac{H^g}{\hbar}\right)\exp\left(-it\frac{H^e}{\hbar}\right)\right\} = \chi^2 < \hat{S}(t)> \tag{A2}$$

Here H^g and H^e are Hamiltonians of spin system in the ground and excited electronic state of the ion. The difference

$$W = H^e - H^g = \hbar\Delta_0 c^+ c, \tag{A3}$$

of spin Hamiltonians describes the interaction which is responsible for optical dephasing. Quantum-statistical average in Eq. (A2) is realized with the following density matrix

$$\hat{\rho}^g(T) = [1 - f_0(T)]cc^+ + f_0(T)c^+c. \tag{A4}$$

Here $f_0(T) = [1 + \exp(\varepsilon/kT)]^{-1}$.

Let us differentiate operator $\hat{S}(t) = \exp\left(it\frac{H^g}{\hbar}\right)\exp\left(-it\frac{H^e}{\hbar}\right)$ in Eq. (A2) with respect to time. We arrive at the following equation:

$$\frac{d}{dt}\hat{S}(t) = -\frac{i}{\hbar}W(t)\hat{S}(t), \tag{A5}$$

Here

$$W(t) = \exp\left(it\frac{H^g}{\hbar}\right)W\exp\left(-it\frac{H^g}{\hbar}\right). \tag{A6}$$

After integration of Eq. (A5) we arrive at the following integral equation:

$$\hat{S}(t) = 1 - \frac{i}{\hbar}\int_0^t dt_1 W(t_1)\hat{S}(t_1). \tag{A7}$$

This operator equation can be solved with the help of iteration procedure. Result looks as follows:

$$\hat{S}(t) = 1 + \sum_{m=1}^{\infty}\left(\frac{-i}{\hbar}\right)^m \int_0^t dt_1 \int_0^{t_1} dt_2 ... \int_0^{t_{m-1}} dt_m W(t_1)W(t_2)... W(t_m) \tag{A8}$$

Integration over times in the right hand side of Eq. (A8) can be simmetrized with the help of so-called time-ordering operator $\widehat{T}$. Result looks as follows

$$<\hat{S}(t)> = 1 + \sum_{m=1}^{\infty}\left(\frac{1}{m!}\right)\left(\frac{-i}{\hbar}\right)^m \int_0^t dt_1 \int_0^t dt_2 ... \int_0^t dt_m \qquad < \widehat{T}\{W(t_1)W(t_2)...\ W(t_m)\}> \tag{A9}$$

Here all times are equal in rights. This fact facilitates our processing of Eq. (A9) after its quantum statistical average.

Consider quantum-statistical average of operator $\hat{S}(t)$. The average can be expressed via so-called cumulant function in the following form:

$$\langle\hat{S}(t)\rangle = \exp g(t), \tag{A10}$$

Here cumulant function g(t) is described by the following expression

$$g(t) = 1 + \sum_{m=1}^{\infty}\left(\frac{1}{m!}\right)\left(\frac{-i}{\hbar}\right)^m \int_0^t dt_1 \int_0^t dt_2 ... \int_0^t dt_m \qquad < \widehat{T}\{W(t_1)W(t_2)...\ W(t_m)\}>_c \tag{A11}$$

Index "c" near sign of the average means that we should take into account only so-called coupled averages of operators. Detailed derivation of Eq. (A10) is presented in Appendix A "Cumulant Expansion" placed in the end of the book [22]. The average of the product in Eq. (A11) can be expressed via product of causal Green functions for spin:

$$G(t) = -i\langle\widehat{T}c(t)c^{+}(0)\rangle = -i\exp\left(-i\frac{\varepsilon}{\hbar}t\right)[(1-f)\theta(t) - f\theta(-t)] \tag{A12}$$

This function doesn't allow for decay of spin state with energy ε. This decay exists in real system and it can be allowed for by introducing decay constant γ into Green function as follows:

$$G(t) = -i\langle\widehat{T}c(t)c^{+}(0)\rangle = -i\exp\left(-i\frac{\varepsilon}{\hbar}t - \gamma t\right)[(1-f)\theta(t) - f\theta(-t)] \tag{A13}$$

By calculating the average in the cumulant function g(t) we arrive at the following expression:

$$g(t) = -\Delta_0 \int_0^t t_1\left\{G(-0) + \sum_{m=2}^{\infty}\frac{{\Delta_0}^{m-1}}{m}\int_0^t dt_2 \int_0^t dt_3 \qquad ... \int_0^t t_m G(t_1 - t_2)...G(t_{m-1} - t_m)\right\} \tag{A14}$$

Carrying out transition to Fourier transforms in the Green functions we arrive at the following equation for cumulant function:

$$g(t) = \sum_{m=1}^{\infty}\frac{\Delta_0^m}{m}\int_{-\infty}^{\infty}\frac{d\omega_1}{2\pi}G(\omega_1)\int_{-\infty}^{\infty}\frac{d\omega_2}{2\pi}G(\omega_2)\ ...\int_{-\infty}^{\infty}\frac{d\omega_m}{2\pi}G(\omega_m)\Delta_t(1-2)\Delta_t(2-3)...\ \Delta_t(m-1) \tag{A15}$$

Here $\Delta_t(k-j) = \sin^2\left(\frac{\omega_k-\omega_j}{2}t\right)/\left(\frac{\omega_k-\omega_j}{2}\right)^2$.

Functions Δ_t are integrated over frequencies in Eq. (A15). At large time we can make the following substitutions

$$\Delta_t(k-j) \to 2\pi\delta(\omega_k - \omega_j),\ \Delta_t(k-j)\Delta_t(j-k) \to |t|2\pi\delta(\omega_k - \omega_j) \tag{A16}$$

in Eq. (A15). Delta functions enable one to make integration over frequencies in Eq. (A15) and we arrive at the following expression for the cumulant function at large time:

$$g_{\infty}(t) = t\left\{\frac{-i\Delta_0}{2} + \int_{-\infty}^{\infty}\frac{d\omega}{2\pi}\sum_{m=1}^{\infty}\frac{1}{m}(\Delta_0 G(\omega))^m\right\} = t\left\{\frac{-i\Delta_0}{2} + \int_{-\infty}^{\infty}\frac{d\omega}{2\pi}\ln(1-\Delta_0 G(\omega))\right\} = t\left\{-i\delta - \frac{\gamma_{e-s}}{2}\right\} \tag{A17}$$

Imaginary part of this function describes a shift of optical line and real part describes contribution to halfwidth of optical line. By using Fourier transform of the Green function in the following form:

$$G(\omega) = \int_{-\infty}^{\infty}\frac{d\nu}{\pi}\quad \Gamma(\nu)\left(\frac{1-f}{\omega-\nu+i0} + \frac{f}{\omega-\nu-i0}\right), \tag{A18}$$

Here function

$$\Gamma(\nu) = \frac{\gamma}{(\nu-\varepsilon)^2 + \gamma^2} \tag{A19}$$

describes spectral density of the spin state at the ground electronic state of Pr^{3+} ion. We can express $\frac{\gamma_{e-s}}{2}$ in the following form [20–22]:

$$\frac{\gamma_{e-s}}{2} = -\int_0^{\infty}\frac{d\nu}{2\pi}\ln[1 - 4f(1-f){\Delta_0}^2\Gamma^e(\nu)\Gamma(\nu)], \tag{A20}$$

Here function

$$\Gamma^e(\nu) = \frac{\Gamma(\nu)}{\left(1 - \Delta_0 P\int_{-\infty}^{\infty}\frac{d\omega}{\pi}\frac{\Gamma(\omega)}{\nu-\omega}\right)^2 + {\Delta_0}^2\Gamma(\nu)^2} \tag{A21}$$

describes spectral density of spin at the excited electronic state of Pr^{3+} ion. Dimensionless parameter Δ_0/γ determines strength of the electron-spin coupling. Therefore we can express Eq. (A21) via dimensionless integral as follows:

$$\frac{\gamma_{e-s}(\chi)}{2} = \gamma I(\chi, \Delta_0/\gamma) \tag{A22}$$

Eq. (A22) describes contribution to optical dephasing from electron-spin interaction.

References

[1] F. Bloch, Phys. Rev. 70 (1946) 460.
[2] L. Allen, J.H. Eberly, Optical Resonance and Two-Level Atoms, Wiley Interscience Publication, NY, 1975.
[3] R.G. DeVoe, R.G. Brewer, Phys. Rev. Lett. 50 (1983) 1269.
[4] M. Weber, J. Chem. Phys. 48 (1968) 4774.
[5] R.M. Macfarlane, R.M. Shelby, R.L. Shoemaker, Phys. Rev. Lett. 43 (1979) 1726.
[6] A. Szabo, T. Muramoto, Phys. Rev. A39 (1989) 3992.
[7] E. Hanamura, J. Phys. Soc. Jpn. 52 (1983) 3678.
[8] M. Yamanoi, J.H. Eberly, Phys. Rev. Lett. 52 (1984) 1353.
[9] M. Yamanoi, J.H. Eberly, J. Opt. Soc. Am. B1 (1984) 751.
[10] J. Javanainen, Opt. Commun. 50 (1984) 261.
[11] A. Schenzle, M. Mitsunaga, R.G. DeVoe, R.G. Brewer, Phys. Rev. A30 (1984) 325.
[12] P.R. Berman, R.G. Brewer, Phys. Rev. A32 (1985) 2784.
[13] K. Wodkiewicz, J.H. Eberly, Phys. Rev. A32 (1985) 992.
[14] P.R. Berman, J. Opt, Soc. Am. B3 (1986) 564.
[15] P.R. Berman, J. Opt, Soc. Am. B3 (1986) 572.
[16] M. Yamanoi, J.H. Eberly, Phys. Rev. A34 (1986) 1609.
[17] A. Szabo, T. Muramoto, Phys. Rev. A37 (1988) 4040.
[18] A. Apanasevich, S.Ya Kilin, A.P. Nizovtsev, N.S. Onishchenko, Opt. Commun. 52 (1984) 279.
[19] S.Ya Kilin, A.P. Nizovtsev, Phys. Rev. A42 (1990) 4403.
[20] I.S. Osad'ko, Chem. Phys. Lett. 115 (1985) 411.
[21] I.S. Osad'ko, Sov. Phys. JETP 63 (1986) 851.
[22] I.S. Osad'ko, Selective Spectroscopy of Single Molecules, Springer, Berlin, 2003.